Philosophical Magazine

ISSN: 1478-6435 (Print) 1478-6443 (Online) Journal homepage: https://www.tandfonline.com/loi/tphm20

Amorphous zirconia: *ab initio* molecular dynamics simulations

Murat Durandurdu

To cite this article: Murat Durandurdu (2017) Amorphous zirconia: *ab initio* molecular dynamics simulations, Philosophical Magazine, 97:16, 1334-1345, DOI: 10.1080/14786435.2017.1296201

To link to this article: https://doi.org/10.1080/14786435.2017.1296201

PHILOSOPHICAL MAGAZINE, 2017
VOL. 97, NO. 16, 1334–1345
http://dx.doi.org/10.1080/14786435.2017.1296201

Taylor & Francis
Taylor & Francis Group

Amorphous zirconia: *ab initio* molecular dynamics simulations

Murat Durandurdu

Department of Materials Science & Nanotechnology Engineering, Abdullah Gül University, Kayseri, Turkey

ABSTRACT

We investigate the short-range order of the liquid and amorphous zirconia using an *ab initio* molecular dynamics technique. Both forms of zirconia are projected to be structurally close to each other. The amorphous network has predominantly seven-fold coordinated Zr atoms (~%65), and three-fold and four-fold coordinated O atoms (~46%), and hence it resembles locally the monoclinic zirconia phase. Within the known limitations of the DFT-GGA calculation, the liquid state is predicted to be semi-metal, whereas the amorphous form is projected to be semiconductor having a band gap energy of ~3.5 eV. We find an asymmetry in localisation of the band tail states. On the basis of this finding, we discuss possible distinctions in n-type and p-type doping in amorphous zirconia.

ARTICLE HISTORY
Received 17 November 2016
Accepted 13 February 2017

KEYWORDS
Zirconia; amorphous; liquid; localisation

Introduction

The amorphous form of zirconia (a-ZrO_2) has some important technological applications, similar to its crystalline phases. It can be used in resistive memory devices, microelectronic devices, flash memory devices, high electron mobility transistors, etc. [1–4]. Due to these important applications, in recent years, there have been some attempts to better understand this material and its physical properties [2,5].

The theoretical studies based on classical molecular dynamics (MD) simulations [6] and first-principles MD calculations [7,8] provided some valuable information regarding the local structure of a-ZrO_2. First-principles MD simulations [7,8] suggested *approximately* the same coordination distributions for a-ZrO_2. Yet because of the small size of the simulation cell, the short simulation time and the statistical assemble used in the first-principles MD simulations, these a-ZrO_2 networks were questioned later [6]. In the classical MD simulations [6], several

CONTACT Murat Durandurdu murat.durandurdu@agu.edu.tr

a-ZrO_2 models were generated using different cooling rates (10^{15}–10^{13} K/s). The coordination distribution of the model constructed using the fastest quenching rate was claimed to be close to the first principles simulations [7,8]. On the other hand, slower cooling rates led to the formation of more seven-fold Zr coordination and three-fold and four-fold O coordination. However, for all cooling rates in the classical MD simulations, the number of six-fold coordinated Zr atoms was predicted to be always higher than that of the seven-fold coordinated Zr atoms in contrast to the first principles MD simulations. Additionally, a close analysis of the partial pair distribution functions (PPDFs) reported in the classical MD simulations (Figure 5 of Ref. [6]) suggested a trivial peak below 2 Å in the O–O correlation, which was, for some reason, not discussed by the authors. This peak means the existence of O–O homopolar bonds in some computer-generated ZrO_2 models. The presence of such O–O bonds was, however, not stated in the first-principles calculations [7,8]. Indeed in oxide materials, the formation of homopolar bonds is generally not anticipated to form due to their high ionicity. Therefore, the readers can query the accuracy of this empirical potential used to model *a*-ZrO_2.

These main differences between the classical and the first-principles MD simulations can depend on some other factors too. For example, the size of the supercell, the time scale of simulation, different statistical assembles used in these simulations and the accuracy of the empirical potential. Although the size can still be an issue for Quantum Mechanical simulations, the influences of the other matters on the atomic structure of *a*-ZrO_2 can be easily addressed at present and the controversies between simulations might be clarified.

In this work, we apply an *ab initio* MD technique to generate an *a*-ZrO_2 model. We also investigate the atomic structure of the liquid ZrO_2. Surprisingly, both states are found to be structurally close to each other. In the amorphous model, about 65% of Zr atoms are seven-fold coordinated and more than 46% of O atoms are three-fold and four-fold coordinated, suggesting the monoclinic-like local structural arrangements in *a*-ZrO_2.

Method

The MD simulation was succeeded by the SIESTA *ab initio* package [9]. We used double-zeta plus polarisation orbitals, the NPT ensemble and Γ-point for the Brillouin zone sampling. Pressure and temperature were controlled by the Parrinelo–Rahman method [10] and the velocity rescaling approach, correspondingly. The generalised gradient approximation (GGA) of Perdew, Burke and Ernzerhof was selected to compute for the exchange-correlation energy [11]. Pseudopotentials were created by the Troullier–Martins scheme [12]. Our earlier works indicated that the parameters (basis, pseudopotentials, etc.) used in the present study were good enough to capture the high-pressure behaviour of the crystalline phases of ZrO_2, and hence they could be safely applied to study the atomic structure of the liquid and amorphous ZrO_2. The high temperature phase of

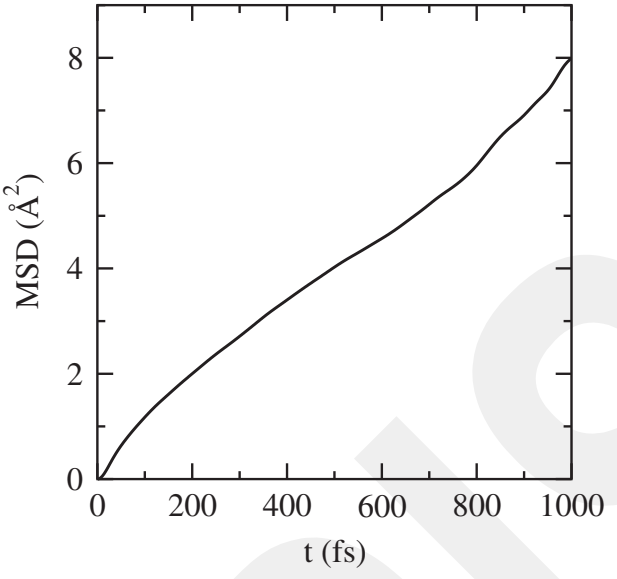

Figure 1. (colour online) Mean square displacement at 3050 K.

ZrO_2, the cubic structure with 144 atoms, was adopted as a starting arrangement. The initial crystal was subjected to 7500 K for 1.0 ps (each MD time step was one femtosecond). Then the structure was cooled down to 3050 K (the melting temperature of ZrO_2 is ~2990 K) in 3.0 ps. At this temperature, the system was poised for about 20.0 ps. In order to confirm that the 20.0 ps was sufficient to capture the dynamics of the liquid state, we run additional 1000 MD steps (constant volume) and studied the mean square displacement (MSD). Figure 1 shows the computed MSD. Beyond 120 fs, the MSD showed a linear behaviour, indicating a diffuse state in the liquid ZrO_2 and its state of equilibrium. The diffusion constant D was estimated to be ~1.05×10^{-4} cm^2/s from a linear fit of the diffusive part (200–600 fs) and the Einstein relation, $\langle (r(t) - r(0))^2 \rangle = 6tD$. After the liquid state at 3050 K was confirmed, the applied temperature was reduced gradually to 300 K in 68.0 ps. The 1000 configurations of the liquid (3050 K) and glass (300 K) states were used for the structural analyses. On the other hand, during the cooling process, a few configurations around some specific temperatures were gathered for the analyses and hence some errors were expected to happen for the data reported between 300 and 3050 K.

Results

The variation of PPDFs with temperature is given in Figure 2. The most apparent alteration is the sharpening of the main peaks with reducing temperature, denoting the propensity of the structure to have a more ordered topology. The Zr–O peak is located around 2.04 Å at 3050 K, sensibly close to the experimental result of

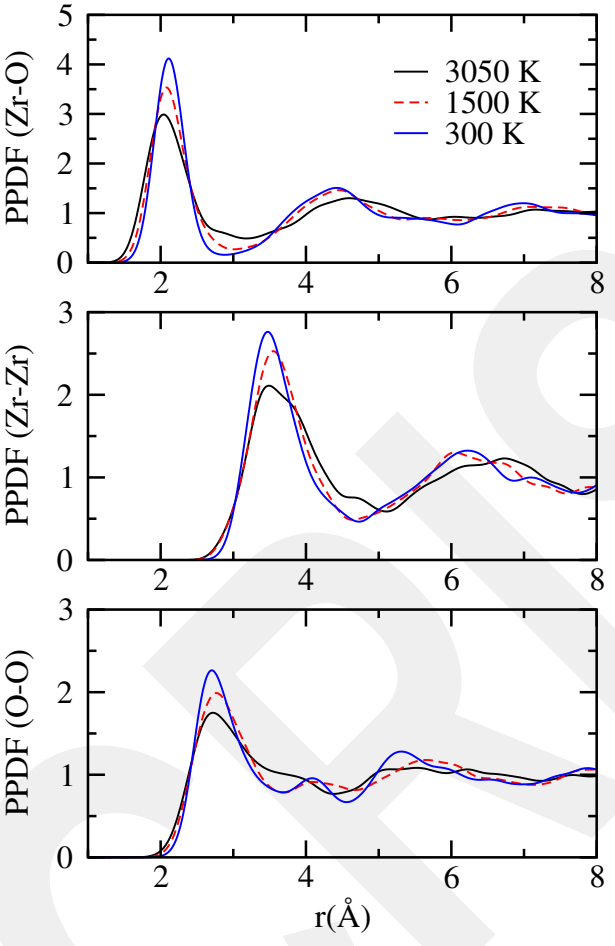

Figure 2. (colour online) Partial pair distribution functions at selected temperatures.

~2.1 Å at 3100 K [13]. The cation–oxygen correlation is 2.11 Å at 300 K, agreeing well with the previous simulation result of 2.11 Å [8]. This finding signifies that the first neighbour bond length is not too sensitive to temperature. The main Zr–Zr peak placed at 3.5 Å in the liquid state appears to be less than the experimental value of ~3.7 Å at 3100 K [13]. The position of this peak is not altered during the quenching process and has a value of ~3.5 Å at 300 K, in accord with the earlier simulation result of 3.50 Å [8]. The main O–O pair at 3050 and 300 K is positioned at 2.72 Å and at 2.70 Å, respectively. The O–O correlation of *a*-ZrO_2 was reported to be at 2.8 Å in Ref. [8], rather comparable with our result. The Zr–O, Zr–Zr and O–O correlations of the high temperature cubic ZrO_2 phase are at ~2.2, 3.62 and 2.55 Å, correspondingly and the monoclinic ZrO_2 phase has these peaks at ~ 2.13, 3.44 and 2.74 Å, respectively. Consequently, one can see that the position of all these peaks is quantitatively captured in our simulations.

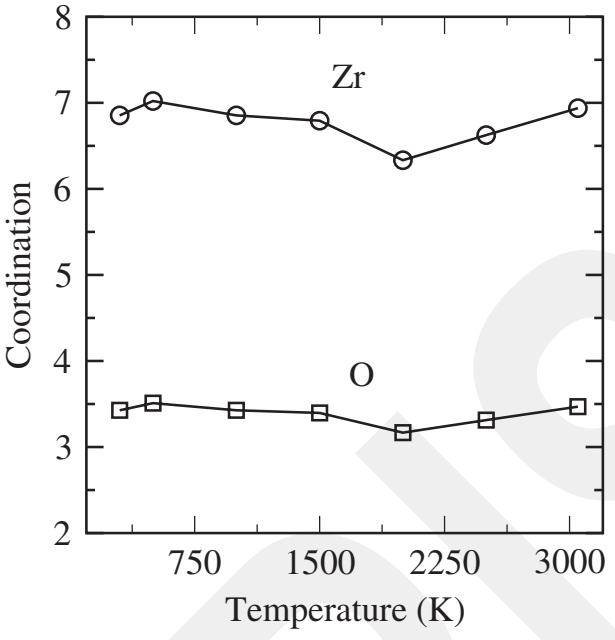

Figure 3. Average coordination number of Zr and O atoms as a function of temperature.

Table 1. Coordination distribution (%) of *a*-ZrO_2 and liquid ZrO_2.

	Ref. [6]	Ref. [7]	Ref. [8]	Ref. [19]	Present (amorphous)	Present (liquid)
O(2)	0.6	3.22	6.45	6.3	4.1	8.3
O(3)	74.2	69.35	64.52	50.0	48.9	43.7
O(4)	24.9	29.03	30.65	40.6	46.8	42.7
O(5)	0.3	1.61	1.61	0	0	3.1
O(6)	0	0	0	0	0	2
Zr(4)	0.2	0	0	0	0	0
Zr(5)	4.2	6.25	18.75	9.3	0	8.3
Zr(6)	48.6	37.5	34.38	18.75	25	18.7
Zr(7)	39.8	50	40.63	56.25	64.5	47.9
Zr(8)	7	6.25	6.25	12.5	10.04	21
Zr(9)	0.2	0	0	3.1	0	4.1

In order to have an additional understanding of the local structure of ZrO_2 phases, we evaluate the coordination distribution using the cutoff radii in the ranges of 3.08 Å (amorphous)-3.18 Å (liquid) for the Zr–O correlation. Figure 3 shows the average O and Zr coordination numbers (CNs) as a function of temperature. The average CNs do not change considerably with temperature. Yet as indicated by Table 1, the coordination distribution is marginally different for the liquid and amorphous structures. In the liquid state, ~21% of Zr atoms are eight-fold or higher coordinated and this fraction drops to ~10% for the amorphous model. The five-fold coordinated Zr atoms (~8%) transform to six-fold coordinated configurations during the cooling process. Note that our amorphous system exhibits the privilege of seven-fold coordinated Zr atoms and an almost

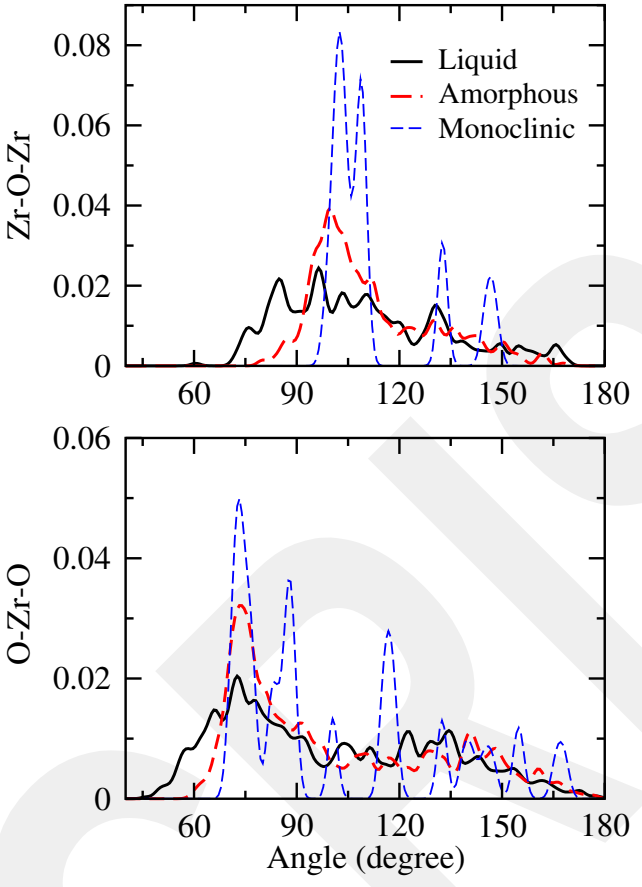

Figure 4. (colour online) Bond angle distribution functions of the liquid, amorphous and monoclinic phases.

equal amount of four-fold and three-fold coordinated O atoms, similar to the monoclinic phase. Additionally, our model is free from five-fold coordinated O and Zr defects. Consequently, it is topologically closer to the monoclinic phase than the previously proposed ones [6–8].

It seems that our liquid state is structurally dissimilar to the earlier predictions [13,14]. The Zr CN of the liquid state in the present work is estimated to be 6.93 that is dramatically higher than the previous MD simulation values of 5.9 [13] and 6.1 [14]. In our liquid system, six-fold, seven-fold and eight-fold coordinated Zr atoms are the leading clusters (see Table 1), while the five-fold, six-fold and seven-fold coordinated units are the most dominant ones in Ref. [13].

Figure 4 shows the Zr–O–Zr and O–Zr–O bond angle distribution functions of the liquid, amorphous and monoclinic phases. The amorphous system has broad distributions ranging from 70° to 170° for the Zr–O–Zr angles and from 45° to 180° for the O–Zr–O angles and a main peak at ~100° and 75° for the Zr–O–Zr and O–Zr–O distributions, respectively. The monoclinic crystal has the Zr–O–Zr angles near 102°, 109°, 133° and 147°, and the O–Zr–O angles around

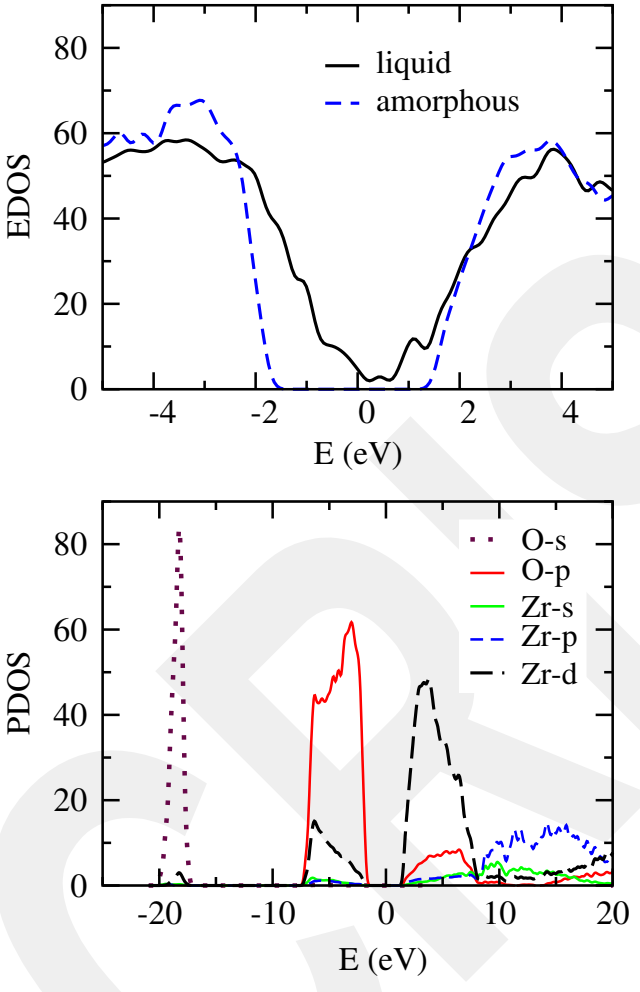

Figure 5. (colour online) Electronic density of states of the liquid and amorphous ZrO_2 (upper panel). Projected density of states of *a*-ZrO_2 (lower panel).

75°, 88°, 100°, 117°, 132°, 140°, 146°, 156° and 168°. Note that the main peaks at 102° and 75° of the monoclinic phase are well-shaped in the amorphous form, suggesting some structural resemblances between these two phases. The cubic crystal produces the O–Zr–O peaks at 70° and 110° with the same magnitude and a weak O–Zr–O peak near 180° and a strong Zr–O–Zr peak at 110°. So one can see the lack of a pronounced peak at these angles in the liquid structure and some likenesses in the angle distributions of the liquid and amorphous phases. Consequently, the local structural arrangement of the liquid state is also predicted to be closer to the monoclinic crystal than the cubic crystal.

The electronic structure of disordered ZrO_2 forms is probed by simply calculating the electron density of states. For the amorphous structure, the HOMO-LUMO band gap energy is estimated to be ~3.5 eV (see Figure 5). This estimation

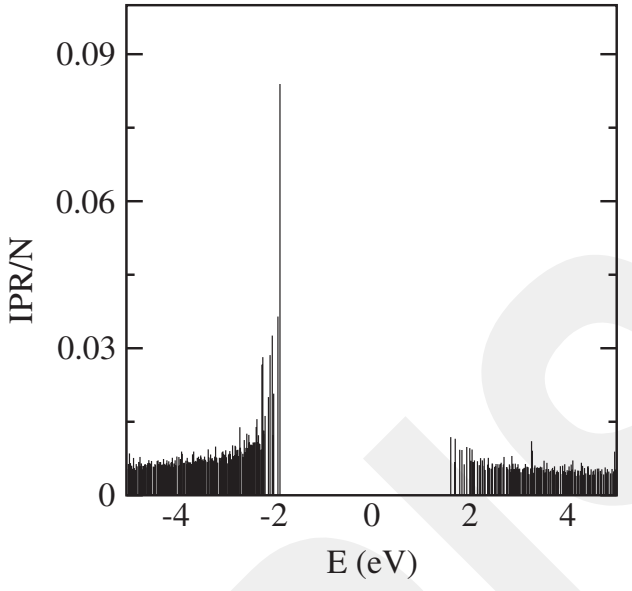

Figure 6. Inverse participation ratio of *a*-ZrO_2.

is comparable with the earlier simulation results of 2.7–3.4 eV [7,8] but it is notably less than the experimental value of 4.7 eV [15], as anticipated because of the self-interaction error in density functional theory (DFT)-GGA calculations. As understood from Figure 5, our DFT-GGA simulation suggests a semi-metallic character for the liquid state. Yet, we are not sure whether this is due to the shortcoming of the DFT-GGA simulation or the true electronic structure of the liquid phase. This can be clarified by experiments or DFT-GGA + U or DFT-GWA calculations. By solely analysing partial electron density of states of the amorphous model, we can see that the conduction band is predominantly due to Zr-d orbitals while the valance band is originated from O-p orbitals (see Figure 5).

The inverse participation ratio ($IPR\left(\psi_j\right) = N\sum_{i=1}^{N} a_i^{j4} / \left(\sum_{i=1}^{N} a_i^{j2}\right)^2$ where $\psi_i = \sum_{i=1}^{N} a_i^j \phi_i$ is the jth eigenstate and N is the number of atoms, see Ref. [16] for more information) is used to extract additional information about the electronic properties of *a*-ZrO_2. Figure 6 shows the estimated IPR. We can see that the valence tails present a higher IPR and thus they are fairly localised. The conduction tail states, on the other hand, have a lower IPR and hence they are weakly localised. So, one can perceive an asymmetry in the localised tail states in *a*-ZrO_2. A similar result was observed for *a*-GaN [16], *a*-SiO_2 and *a*-SnO_2 [17]. Using the asymmetric localisation of the tail states, possible distinctions in n-type and p-type doping for these materials were speculated in these studies [16,17]. Using the same assumption, we can also propose that because of the localisation of the valence tail states, it would be hard to shift the Fermi level to the valence band and the mobility is likely insignificant. Consequently, the p-type doping is anticipated

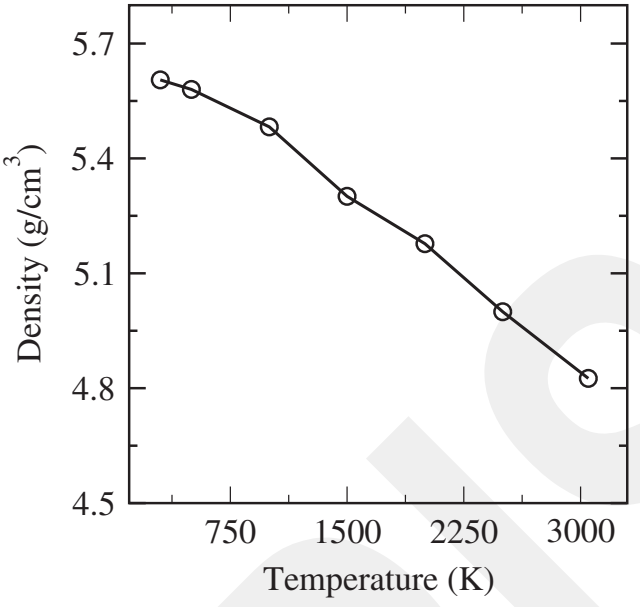

Figure 7. Variation of the density as a function of temperature.

to be harder than n-type doping to achieve an equivalent carrier concentration for *a*-ZrO_2.

Discussion

The present study offers a rather different local picture for *a*-ZrO_2 than the earlier first principles MD simulations [7,8] and the empirical potential investigation [6]. Relative to them, our model is locally closer to the monoclinic crystal. This distinction might be connected to the time scale, statistical assembles, the accuracy of the classical potential, etc. used in these simulations. Our simulation time is reasonably longer than the previous first principles MD studies. Also, we used the NPT ensemble instead of NVT, in which the statistical fluctuation of the volume was allowed. Figure 7 shows the modification of the density of ZrO_2 with temperature. The density of the liquid state at 3050 K is estimated to be 4.82 g/cm^3 (0.071 atoms/Å^3), which is fairly close to the experimental density, 0.0733 atoms/Å^3 at 3100 K [13]. As the applied temperature is reduced, the density increases progressively and reaches a value of 5.6049 g/cm^3 at 300 K, which is indeed rather higher than the density, 5.32 g/cm^3 [8] and 4.86 g/cm^3 [7] used to model *a*-ZrO_2 in the earlier investigations. Consequently, the higher density of our model leads probably to more seven-fold coordinated Zr atoms and four-fold coordinated O atoms, relative to the other models [7,8]. We need to point out here that the experimental density of the monoclinic ZrO_2 phase is 5.68 g/cm^3, which is reasonably comparable with the density of our amorphous model.

Vanderbit's group used the SIEST-A-RT [activation relaxation technique (ART) [18] implemented in SIESTA *ab initio* code] method to understand the influence of the fast cooling rate used in the MD simulations on the local structure of *a*-ZrO_2 [19,20]. The coordination distribution of this model (roughly predicted from the Figure 4 of Ref. [19]) is also provided in the Table 1. In their SIEST-A-RT model, similar to ours, almost the same amount of four-fold and three-fold coordinated O atoms is observed. Since the ART is applied to investigate the long time dynamics of amorphous networks and to contsruct realistic amorphous models, the *striking* resemblances between our model and the SIEST-A-RT model indicate that the long-time dynamic of *a*-ZrO_2 was fairly captured in our MD simulation.

We need to point out here that the dielectric properties of the SIEST-A-RT network were predicted to be close to those of the monoclinic ZrO_2 phase [20], endorsing that it actually represents qualitative features of *a*-ZrO_2, and hence our model considering their obvious similarities.

As reviewed above, the present study and Ref. [13] propose a distinct short-range order for the liquid ZrO_2. Indeed, the density of liquid ZrO_2 used in Ref. [13] is the experimental density, 0.0733 atoms/$Å^3$ [13] and it is relatively close to what has been found in our simulation. Furthermore, the Zr–O bond distance predicted in both simulations is also comparable [13]. Therefore, it is hard to have a clear explanation about the controversy between the present study and Ref. [13] regarding the local structure of the liquid state. Yet, two major differences between these two simulations, the statistical assembles (NPT vs. NVT) and basis set (localised atomic orbitals vs. localised Gaussian and plane wave basis sets), might be responsible for the dissimilar observation.

Conclusions

The atomic and electronic structures of the liquid and amorphous ZrO_2 are explored by means of *ab initio* MD calculations. Noticeable structural resemblances between the liquid and amorphous states are revealed. Zr atoms mainly structure in seven-fold coordinated clusters, whereas O atoms form three-fold and four-fold coordinated configurations in *a*-ZrO_2 and thus its short-range order is close to that of the monoclinic phase. Within the limitations of the DFT-GGA calculation, it is found that the liquid state is a semi-metal, while the amorphous form exhibits a semiconducting behaviour with a clear band energy of about 3.5 eV. Furthermore, the electronic structure calculations suggest localised valence tail states and hence n-type doping is proposed to be easier than the p-type doping in *a*-ZrO_2.

Acknowledgement

The calculations were partially run on TÜBİTAK ULAKBİM, High Performance and Grid Computing Center (TRUBA resources).

Disclosure statement

No potential conflict of interest was reported by the author.

Funding

This work was supported by the Abdullah Gül University Support Foundation.

References

[1] D. Panda and T.Y. Tseng, *Growth, dielectric properties, and memory device applications of ZrO2 thin films*, Thin Solid Films 531 (2013), pp. 1–20.
[2] P. Parreira, G.W. Paterson, S. McVitie, and D.A. MacLaren, *Stability, bistability and instability of amorphous ZrO 2 resistive memory devices*, J. Phys. D: Appl. Phys 49 (2016), pp. 095111–095116.
[3] A. Kumar, S. Mondal, and K.S.R. Rao, *Low temperature solution processed high-κ ZrO2 gate dielectrics for nanoelectronics*, Appl. Surf. Sci 370 (2016), pp. 373–379.
[4] G. Ye, H. Wang, S. Arulkumaran, G.I. Ng, R. Hofstetter, Y. Li, M.J. Anand, K.S. Ang, Y.K.T. Maung, and S.C. Foo, *Atomic layer deposition of ZrO 2 as gate dielectrics for AlGaN/GaN metal-insulator-semiconductor high electron mobility transistors on silicon*, Appl. Phys. Lett 103 (2013), pp. 142109–142111.
[5] A. Hojabri, *Structural and optical characterization of ZrO2 thin films grown on silicon and quartz substrates*, J. Theor. Appl. Phys. 10 (2016), pp. 1–6.
[6] S.A. Arash Sheikholeslam, G.M. Xia, C. Grecu, and A. Ivanov, *Generation and properties of bulk a-ZrO2 by molecular dynamics simulations with a reactive force field*, Thin Solid Films 594 (2015), pp. 172–177.
[7] X. Zhao, D. Ceresoli, and D. Vanderbilt, *Structural, electronic, and dielectric properties of amorphous Zr O 2 from ab initio molecular dynamics*, Phys. Rev. B 71 (2005), pp. 085107–085116.
[8] E.A. Chagarov and A.C. Kummel, *Generation of realistic amorphous Al2O3 And ZrO2 samples by hybrid classical and first-principle molecular dynamics simulations*, ECS Trans. 16 (2008), pp. 773–785.
[9] P. Ordejón, E. Artacho, and J.M. Soler, *Self-consistent order-N density- functional calculations for very large systems*, Physical Review B 53 (1996), pp. R10441–R10444.
[10] M. Parrinello and A. Rahman, *Polymorphic transitions in single crystals: A new molecular dynamics method*, J. Appl. Phys. 52 (1981), pp. 7182–7190.
[11] J.P. Perdew, K. Burke, and M. Ernzerhof, Generalized gradient approximation made simple, Phys. Rev. Lett. 77 (1996), pp. 3865–3868.
[12] N. Troullier and J.M. Martins, *Efficient pseudopotentials for plane-wave calculations*, Phys. Rev. B 43 (1991), pp. 1993–2006.
[13] S. Kohara, J. Akola, L. Patrikeev, M. Ropo, K. Ohara, M. Itou, A. Fujiwara, J. Yahiro, J.T. Okada, T. Ishikawa, A. Mizuno, A. Masuno, Y. Watanabe, and T. Usuki, *Atomic and electronic structures of an extremely fragile liquid*, Nat, Commun. 5 (2014), p. 5892.
[14] L.B. Skinner, C.J. Benmore, J.K.R. Weber, J. Du, J. Neuefeind, S.K. Tumber, and J.B. Parise, Low cation coordination in oxide melts, Phys. Rev. Lett. 112 (2014), pp. 157801–157805.
[15] V. Gritsenko, D. Gritsenko, S. Shaimeev, V. Aliev, K. Nasyrov, S. Erenburg, V. Tapilin, H. Wong, M.C. Poon, J.H. Lee, J.W. Lee, and C.W. Kim, *Atomic and electronic structures of amorphous ZrO2 and HfO2 films*, Microelectron. Eng. 81 (2005), pp. 524–529.

[16] B. Cai and D.A. Drabold, *Properties of amorphous GaN from first-principles simulations*, Phys. Rev. B 84 (2011), pp. 075216–075221.
[17] J. Robertson, *Physics of amorphous conducting oxides*, J. Non-Cryst. Solids 354 (2008), pp. 2791–2795.
[18] G.T. Barkema and N. Mousseau, Event-based relaxation of continuous disordered systems, Phys. Rev. Lett. 77 (1996), pp. 4358–4361.
[19] D. Vanderbilt, X. Zhao, and D. Ceresoli, *Structural and dielectric properties of crystalline and amorphous ZrO2*, Thin Solid Films 486 (2005), pp. 125–128.
[20] D. Ceresoli and D. Vanderbilt, *Structural and dielectric properties of amorphous ZrO 2 and HfO 2*, Phys. Rev. B 74 (2006), pp. 125108–125113.